

Measurement of the neutrino magnetic moment at the NOvA experiment

Technical note

Robert Kralik¹

¹University of Sussex, Brighton, UK

November 28, 2023

Abstract

This is the abstract

Contents

1	Introduction	4
2	Literature review	4
2.1	Theoretical overview	4
2.2	Electromagnetic properties of the neutrino	5
2.2.1	Neutrino electric and magnetic dipole moments	6
2.3	Measuring neutrino magnetic moment	8
2.3.1	Effective neutrino magnetic moment	8
2.3.2	Neutrino-on-electron elastic scattering	8
2.4	Experimental overview	12
2.5	Direct muon (anti)neutrino magnetic moment measurements	13
2.5.1	NOvA (Biao's thesis)	13
2.5.2	MiniBooNE	13
2.5.3	E734 at the Alternating Gradient Synchrotron (AGS) of the Brookhaven National Laboratory	13
2.5.4	LSND	13
2.6	Direct electron (anti)neutrino magnetic moment measurements	13
2.7	Solar neutrino magnetic moment measurements	13
2.7.1	XENONnT	13
2.7.2	XENON1T	14
2.7.3	BOREXINO	14
2.7.4	GEMMA	14
2.8	Other	14
2.8.1	LHC Forward Physics Facilities	14
2.9	Astrophysics	16
3	Analysis overview	17
3.1	Datasets and Event Reconstruction details	17
3.1.1	Enhanced ν -on-e sample	17
3.1.2	Enhance ν_e CC MEC sample	17
3.2	Analysis weights	17
3.2.1	Neutrino magnetic moment as a weight	17
3.2.2	Radiative correction weight	17
3.3	Event selection	17
3.4	Resolution and binning	17
3.4.1	Fitting framework	17
4	Systematic uncertainties	17
4.1	Normalization systematics	17
4.2	Neutrino flux systematics	17
4.3	Detector systematics	18

4.4	Cross section systematics	18
5	Results	18
5.1	Counting experiment	18
5.2	Binned experiment	18
5.2.1	Sensitivities and limits	18
6	Conclusion	18

1 Introduction

Main motivations for the analysis. Briefly mention that there was a previous study by Biao, what were the results there and what limitations (or maybe talk about this in the Experimental overview?).

Maybe briefly mention the overview of the theory and experimental overview.

2 Literature review

2.1 Theoretical overview

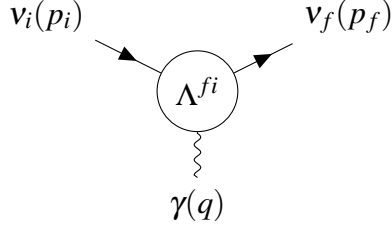


Figure 1: Effective coupling of neutrinos with one photon electromagnetic field.

2.2 Electromagnetic properties of the neutrino

In the standard model, neutrino can have electromagnetic interaction only at a higher order of the perturbative expansion of the interaction - from loop diagrams.

In the one photon approximation, the electromagnetic interactions of a neutrino field ($v_k(x), k \in \{1, \dots, N\}$), for N neutrino mass states, can be described by the effective interaction Hamiltonian [?]

$$\mathcal{H}_{em}^{(v)}(x) = \sum_{k,j=1}^N \bar{v}_k(x) \Lambda_\mu^{kj} v_j(x) A^\mu(x) \quad (1)$$

and the amplitude of neutrino-to-neutrino interaction for **Dirac** neutrinos shown on fig.1 is

$$\langle v_f(p_f) | j_\mu^{(v)}(x) | v_i(p_i) \rangle = e^{i(p_f - p_i)x} \bar{u}_f(p_f) \Lambda_\mu^{fi}(p_f, p_i) u_i(p_i), \quad (2)$$

where p_f and p_i are the final and initial four momentums respectively and u/\bar{u} are the solutions to the Dirac equation for a free particle. We take into account possible transitions between different mass states v_i and v_f [?].

The vertex function $\Lambda_\mu^{fi}(p_f, p_i)$ is a matrix and in the most general case it can be written in terms of linearly independent products of Dirac matrices (γ) and four momentum of the photon ($q = p_f - p_i$):

$$\begin{aligned} \Lambda_\mu^{fi}(p_f, p_i) = & \mathbb{F}_1^{fi}(q^2) q_\mu + \mathbb{F}_2^{fi}(q^2) q_\mu \gamma_5 + \mathbb{F}_3^{fi}(q^2) \gamma_\mu + \mathbb{F}_4^{fi}(q^2) \gamma_\mu \gamma_5 + \\ & \mathbb{F}_5^{fi}(q^2) \sigma_{\mu\nu} q^\nu + \mathbb{F}_6^{fi}(q^2) \varepsilon_{\mu\nu\rho\gamma} q^\nu \sigma^{\rho\gamma}, \end{aligned} \quad (3)$$

where $\mathbb{F}_i^{fi}(q^2)$ are six Lorentz invariant form factors. For $f = i$ they are called "diagonal" and for $f \neq i$ "transition form factors" [?].

Applying conditions of hermiticity ($\mathcal{H}_{em}^{(v)\dagger} = \mathcal{H}_{em}^{(v)}$) and of conservation of the current (continuity equation: $\partial^\mu j_\mu^{(v)}(x) = 0$), we can rewrite the vertex function as

$$\Lambda_\mu^{fi}(q) = (\gamma_\mu - q_\mu \not{q} / q^2) \left[\mathbb{F}_Q^{fi}(q^2) + \mathbb{F}_A^{fi}(q^2) q^2 \gamma_5 \right] - i \sigma_{\mu\nu} q^\nu \left[\mathbb{F}_M^{fi}(q^2) + i \mathbb{F}_E^{fi}(q^2) \gamma_5 \right], \quad (4)$$

where $\mathbb{F}_Q^{fi}, \mathbb{F}_M^{fi}, \mathbb{F}_E^{fi}$ and \mathbb{F}_A^{fi} are hermitian matrices representing the real charge, dipole magnetic, dipole electric and anapole neutrino form factors. In coupling with a real photon ($q^2 = 0$) these become the neutrino charge, magnetic, electric and anapole moment [?].

For antineutrinos the form factors are transformed as:

$$\bar{\mathbb{F}}_{\Omega}^{fi} = -\mathbb{F}_{\Omega}^{if} = -\left(\mathbb{F}_{\Omega}^{fi}\right)^{\star} \quad \Omega = Q, M, E, \quad (5)$$

$$\bar{\mathbb{F}}_A^{fi} = \mathbb{F}_A^{if} = \left(\mathbb{F}_A^{fi}\right)^{\star}. \quad (6)$$

In case of **Majorana neutrinos**, the general expression for the vertex function in terms of charge, magnetic, electric and anapole form factors looks the same as for Dirac neutrinos. However, since Majorana antineutrinos are the same particle as Majorana neutrinos, from eq.5,6 we can see that:

$$\mathbb{F}_{\Omega}^M = -\left(\mathbb{F}_{\Omega}^M\right)^T \quad \Omega = Q, M, E, \quad (7)$$

$$\mathbb{F}_A^M = \left(\mathbb{F}_A^M\right)^T. \quad (8)$$

Therefore the Majorana charge, magnetic and electric form factor matrices are antisymmetric and the anapole form factor matrix is symmetric. This means that Majorana neutrino doesn't have any diagonal charge and dipole magnetic and electric moments, but it can have transition charge and magnetic and electric moment [?].

[NuMMBasicsAndAstro_2022.pdf] One of the most important for astrophysics consequences of neutrino nonzero effective magnetic moments is the neutrino helicity change $\nu_l \rightarrow \nu_R$ with the appearance of nearly sterile right-handed neutrinos ν_R . In general, this phenomena can proceed in three different mechanisms:

1. the helicity change in the neutrino magnetic moment scattering on electrons (or protons and neutrons),
2. the neutrino spin and spin-flavour precession in an external magnetic field, and
3. the neutrino spin and spin-flavour precession in the transversally moving matter currents or in the transversally polarized matter at rest

For completeness note that the important astrophysical consequence of nonzero neutrino millicharges is the neutrino deviation from the rectilinear trajectory.

2.2.1 Neutrino electric and magnetic dipole moments

Evaluating the one loop diagrams in the minimal extension of the standard model with right handed (Dirac) neutrinos gives us the first approximation of the electric and magnetic moments ($q^2 = 0$):

$$\left. \begin{matrix} \mu_{kj}^D \\ i\varepsilon_{kj}^D \end{matrix} \right\} \simeq \frac{3eG_F}{16\sqrt{2}\pi^2} (m_k \pm m_j) \left(\delta_{kj} - \frac{1}{2} \sum_{l=e,\mu,\tau} U_{lk}^{\star} U_{lj} \frac{m_l^2}{m_W^2} \right), \quad (9)$$

where m_k, m_j are the neutrino masses, but m_l are the masses of charged leptons which appear in the loop diagrams. Higher order electromagnetic corrections were neglected, but those can also have a significant contribution [?].

There are no diagonal electric moments ($\epsilon_{kk}^D = 0$) and the diagonal magnetic moments are approximately

$$\mu_{kk}^D \simeq \frac{3eG_F m_k}{8\sqrt{2}\pi^2} \simeq 3.2 \times 10^{-19} \left(\frac{m_k}{\text{eV}}\right) \mu_B, \quad (10)$$

where μ_B is the Bohr magneton [?].

The transition magnetic moments are suppressed with respect to the largest of the diagonal magnetic moments by at least a factor of 10^{-4} due to the m_W^2 in denominator and the transition electric moments are even smaller than that due to the mass difference [?]. Therefore an experimental observation of a magnetic moment larger than in eq.10 would indicate physics beyond the minimally extended standard model [?].

Majorana neutrinos can be obtained by either adding a $SU(2)_L$ Higgs triplet, or right handed neutrinos together with a $SU(2)_L$ Higgs singlet. If we neglect the Feynman diagrams which depend on the model of the scalar sector, the magnetic and electric dipole moments are

$$\mu_{kj}^M \simeq -\frac{3ieG_F}{16\sqrt{2}\pi^2} (m_k + m_j) \sum_{l=e,\mu,\tau} \text{Im}[U_{lk}^* U_{lj}] \frac{m_l^2}{m_W^2}, \quad (11)$$

$$\epsilon_{kj}^M \simeq \frac{3ieG_F}{16\sqrt{2}\pi^2} (m_k - m_j) \sum_{l=e,\mu,\tau} \text{Re}[U_{lk}^* U_{lj}] \frac{m_l^2}{m_W^2}. \quad (12)$$

These are difficult to compare to the Dirac case, due to possible presence of Majorana phases in the PMNS matrices, but it is clear that they have the same order of magnitude as Dirac transition dipole moments. However, the neglected model dependent contributions can enhance the transition dipole moments [?].

It is possible [?] to obtain "natural" upper limits on the size of neutrino magnetic moment by calculating its contribution to the neutrino mass by standard model radiative corrections. For Dirac neutrinos the radiative correction induced by neutrino magnetic moment, generated at an energy scale Λ , to the neutrino mass is generically

$$m_\nu^D \sim \frac{\mu_\nu^D}{3 \times 10^{-15} \mu_B} [\Lambda (\text{TeV})]^2 \text{eV}. \quad (13)$$

So for $\Lambda \simeq 1 \text{TeV}$ and $m_\nu \lesssim 0.3 \text{eV}$ the limit becomes $\mu_\nu^D \lesssim 10^{-15} \mu_B$. This applies only if the new physics is well above the electroweak scale ($\Lambda_{EW} \sim 100 \text{GeV}$). It is possible to get Dirac neutrino magnetic moment higher than this limit, for example in frameworks of minimal super-symmetric standard model, by adding more Higgs doublets, or by considering large extra dimensions [?].

The limit for Majorana neutrino magnetic moment is less stringent, due to the antisymmetry condition from eq.7 and considering $m_\nu \lesssim 0.3 \text{eV}$ can be expressed as

$$\mu_{\tau\mu}, \mu_{\tau e} \lesssim 10^{-9} [\Lambda (\text{TeV})]^{-2} \quad (14)$$

$$\mu_{\mu e} \lesssim 3 \times 10^{-7} [\Lambda (\text{TeV})]^{-2} \quad (15)$$

which is shown in the flavour basis, which relates to the framework used previously as

$$\mu_{ij} = \sum_{\alpha\beta} \mu_{\alpha\beta} U_{\alpha i}^* U_{\beta j}, \quad \alpha, \beta \in \{e, \mu, \tau\}. \quad (16)$$

This limits imply, that if a magnetic moment $\mu \gtrsim 10^{-15} \mu_B$ would be measured, it is plausible neutrinos are Majorana fermions and the scale of lepton violation would be well below the conventional see-saw scale [?].

2.3 Measuring neutrino magnetic moment

2.3.1 Effective neutrino magnetic moment

What we measure in experiments is an effective "flavour" magnetic moment, which is influenced by mixing of "mass" magnetic moments (and electric moments) and oscillations. In the ultrarelativistic limit this is

$$\mu_{\nu_l}^2(L, E_\nu) = \sum_j \left| \sum_k U_{lk}^* e^{-i\Delta m_{kj}^2 L/2E_\nu} (\mu_{jk} - i\varepsilon_{jk}) \right|^2. \quad (17)$$

What is called the effective magnetic moment (often just magnetic moment) therefore contains contributions from both the neutrino magnetic and electric moment [?].

For antineutrinos, the effective magnetic moment is

$$\mu_{\bar{\nu}_l}^2(L, E_\nu) = \sum_j \left| \sum_k U_{lk}^* e^{+i\Delta m_{kj}^2 L/2E_\nu} (\mu_{jk} - i\varepsilon_{jk}) \right|^2. \quad (18)$$

So the only difference is in the phase induced by neutrino oscillations.

For experiments with baselines short enough for neutrino oscillations to not develop ($\frac{\Delta m^2 L}{2E_\nu} \ll 1$), such as the NOvA ND, the effective magnetic moment can be expressed as

$$\mu_{\nu_l}^2 \simeq \mu_{\bar{\nu}_l}^2 \simeq \sum_j \left| \sum_k U_{lk}^* (\mu_{jk} - i\varepsilon_{jk}) \right|^2 = \left[U (\mu^2 + \varepsilon^2) U^\dagger + 2\text{Im} \left(U \mu \varepsilon U^\dagger \right) \right]_{ll'}, \quad (19)$$

which is independent of the neutrino energy and of the source to detector distance.

It is important to mention, that since the effective magnetic moment depends on the flavour of the studied neutrino, it is different for different types of neutrino experiment. Also the solar neutrino experiments need to include the effect of the solar matter on the neutrino oscillations. Therefore the reports on the value (or upper limit) of the effective neutrino magnetic moment are not directly comparable between different types of neutrino experiments.

2.3.2 Neutrino-on-electron elastic scattering

The most sensitive method to measure neutrino magnetic moment is the low energy elastic scattering of (anti)neutrinos on electrons [?]. This interaction has two observables, the recoil electron's kinetic energy (T_e) and the recoil angle with respect to the incoming neutrino beam (θ). From simple $2 \rightarrow 2$ kinematics we can get

$$(P_\nu - P_{e'})^2 = (P_{\nu'} - P_e)^2, \quad (20)$$

$$m_{\nu}^2 + m_e^2 - 2E_{\nu}E_{e'} + 2E_{\nu}p_{e'} \cos \theta = m_{\nu}^2 + m_e^2 - 2E_{\nu'}m_e. \quad (21)$$

Using the energy conservation

$$E_{\nu} + m_e = E_{\nu'} + E_{e'} = E_{\nu'} + T_e + m_e \Rightarrow E_{\nu'} = E_{\nu} - T_e \quad (22)$$

we get

$$E_{\nu}p_{e'} \cos \theta = E_{\nu}E_{e'} - E_{\nu'}m_e = E_{\nu}(T_e + m_e) - (E_{\nu} - T_e)m_e = T_e(E_{\nu} + m_e), \quad (23)$$

$$\cos \theta = \frac{E_{\nu} + m_e}{E_{\nu}} \sqrt{\frac{T_e^2}{E_{e'}^2 - m_e^2}} = \frac{E_{\nu} + m_e}{E_{\nu}} \sqrt{\frac{T_e^2}{T_e^2 + 2T_em_e}}. \quad (24)$$

And finally we get

$$\cos \theta = \frac{E_{\nu} + m_e}{E_{\nu}} \sqrt{\frac{T_e}{T_e + 2m_e}}. \quad (25)$$

Electron's kinetic energy is kinematically constrained by

$$T_e \leq \frac{2E_{\nu}^2}{2E_{\nu} + m_e}. \quad (26)$$

Considering $E_{\nu} \sim \text{GeV}$, we can approximate $\frac{m_e^2}{E_{\nu}^2} \rightarrow 0$ and in the small angle approximation we get from eq.25

$$T\theta^2 \cong 2m_e \left(1 - \frac{T_e}{E_{\nu}}\right) < 2m_e. \quad (27)$$

In the ultrarelativistic limit, the neutrino magnetic moment changes the neutrino helicity, turning active neutrinos into sterile. Since the SM weak interaction conserves helicity we can add the two contribution to the neutrino on electron cross section incoherently [?]:

$$\frac{d\sigma_{\nu_l e^-}}{dT_e} = \left(\frac{d\sigma_{\nu_l e^-}}{dT_e}\right)_{\text{SM}} + \left(\frac{d\sigma_{\nu_l e^-}}{dT_e}\right)_{\text{MAG}}. \quad (28)$$

The standard model contribution can be expressed as [?]:

$$\left(\frac{d\sigma_{\nu_l e^-}}{dT_e}\right)_{\text{SM}} = \frac{G_F^2 m_e}{2\pi} \left\{ (g_V^{\nu_l} + g_A^{\nu_l})^2 + (g_V^{\nu_l} - g_A^{\nu_l})^2 \left(1 - \frac{T_e}{E_{\nu}}\right)^2 + \left((g_A^{\nu_l})^2 - (g_V^{\nu_l})^2\right) \frac{m_e T_e}{E_{\nu}^2} \right\}, \quad (29)$$

where the coupling constants g_V and g_A are different for different neutrino flavours and for antineutrinos. Their values are:

$$g_V^{\nu_e} = 2\sin^2 \theta_W + 1/2, \quad g_A^{\nu_e} = 1/2, \quad (30)$$

$$g_V^{\nu_{\mu, \tau}} = 2\sin^2 \theta_W - 1/2, \quad g_A^{\nu_{\mu, \tau}} = -1/2. \quad (31)$$

For antineutrinos $g_A \rightarrow -g_A$.

Using expressions 25 and 27 we can also derive [?] cross sections with respect to $\cos \theta$, θ^2 and $T\theta^2$:

$$\left(\frac{d\sigma_{\nu_l e^-}}{d\cos\theta}\right)_{\text{SM}} = \frac{2G_F^2 E_\nu^2 m_e^2 \cos\theta (E_\nu + m_e)^2}{\pi \left((E_\nu + m_e)^2 - E_\nu^2 \cos^2\theta\right)^2} \left\{ (g_V^{\nu_l} + g_A^{\nu_l})^2 + (g_V^{\nu_l} - g_A^{\nu_l})^2 \left(1 - \frac{2m_e E_\nu \cos^2\theta}{(E_\nu + m_e)^2 - E_\nu^2 \cos^2\theta}\right)^2 + \left((g_A^{\nu_l})^2 - (g_V^{\nu_l})^2\right) \frac{2m_e^2 \cos^2\theta}{\left((E_\nu + m_e)^2 - E_\nu^2 \cos^2\theta\right)} \right\}, \quad (32)$$

$$\left(\frac{d\sigma_{\nu_l e^-}}{d\theta^2}\right)_{\text{SM}} = \frac{G_F^2 m_e^2}{\pi \left(\theta^2 + \frac{2m_e}{E_\nu}\right)^2} \left\{ (g_V^{\nu_l} + g_A^{\nu_l})^2 + (g_V^{\nu_l} - g_A^{\nu_l})^2 \left(\frac{\theta^2}{\theta^2 + \frac{2m_e}{E_\nu}}\right)^2 + \left((g_A^{\nu_l})^2 - (g_V^{\nu_l})^2\right) \frac{2m_e^2}{E_\nu^2 \left(\theta^2 + \frac{2m_e}{E_\nu}\right)} \right\}, \quad (33)$$

$$\left(\frac{d\sigma_{\nu_l e^-}}{dT\theta^2}\right)_{\text{SM}} = \frac{G_F^2 E_\nu}{4\pi} \left\{ (g_V^{\nu_l} + g_A^{\nu_l})^2 + (g_V^{\nu_l} - g_A^{\nu_l})^2 \left(\frac{T\theta^2}{2m_e}\right)^2 + \left((g_A^{\nu_l})^2 - (g_V^{\nu_l})^2\right) \frac{m_e}{E_\nu} \left(1 - \frac{T\theta^2}{2m_e}\right) \right\}. \quad (34)$$

The neutrino magnetic moment contribution is (include derivation from [?]) [?]:

$$\left(\frac{d\sigma_{\nu_l e^-}}{dT_e}\right)_{\text{MAG}} = \frac{\pi\alpha^2}{m_e^2} \left(\frac{1}{T_e} - \frac{1}{E_\nu}\right) \left(\frac{\mu_{\nu_l}}{\mu_B}\right)^2, \quad (35)$$

where α is the fine structure constant.

Analogically to previous, we can also express this cross section in $\cos \theta$, θ^2 and $T\theta^2$:

$$\left(\frac{d\sigma_{\nu_l e^-}}{d\cos\theta}\right)_{\text{MAG}} = \frac{2\pi\alpha^2 (E_\nu + m_e)^2 (E_\nu + m_e)^2 - E_\nu^2 \cos^2\theta - 2m_e E_\nu \cos^2\theta}{m_e^2 \cos\theta \left((E_\nu + m_e)^2 - E_\nu^2 \cos^2\theta\right)^2} \left(\frac{\mu_{\nu_l}}{\mu_B}\right)^2, \quad (36)$$

$$\left(\frac{d\sigma_{\nu_l e^-}}{d\theta^2}\right)_{\text{MAG}} = \frac{\pi\alpha^2}{m_e^2} \frac{\theta^2}{\left(\theta^2 + \frac{2m_e}{E_\nu}\right)} \left(\frac{\mu_{\nu_l}}{\mu_B}\right)^2, \quad (37)$$

$$\left(\frac{d\sigma_{\nu_l e^-}}{dT\theta^2}\right)_{\text{MAG}} = \frac{\pi\alpha^2}{4m_e^4} \frac{T\theta^2}{\left(1 - \frac{T\theta^2}{2m_e}\right)} \left(\frac{\mu_{\nu_l}}{\mu_B}\right)^2. \quad (38)$$

The magnetic moment contribution exceeds the standard model contribution for low enough T_e [?]:

$$T_e \lesssim \frac{\pi^2\alpha^2}{G_F^2 m_e^3} \left(\frac{\mu_\nu}{\mu_B}\right)^2 \simeq 2.9 \times 10^{19} \left(\frac{\mu_\nu}{\mu_B}\right)^2 [\text{MeV}], \quad (39)$$

which does not depend on the neutrino energy and makes neutrino experiment sensitive to lower energetic neutrinos more sensitive to the neutrino magnetic moment.

2.4 Experimental overview

2.5 Direct muon (anti)neutrino magnetic moment measurements

2.5.1 NOvA (Biao's thesis)

- ν_μ only
- Only comparing total event counts - 25 events observed and 23.78 expected
- Put an upper limit (90% C.L.) of $\mu_{\nu_\mu} < 1.58 \times 10^{-9} \mu_B$ with 10.9% systematic uncertainty on the standard model background
- Used 3.62×10^{20} POT of data (6.74×10^{23} POT for MC) with $T\theta^2 < 0.003 \text{ GeV} \times \text{Rad}^2$, $0.3 < T < 0.9 \text{ GeV}$

2.5.2 MiniBooNE

- ν_μ only
- Observed excess of events (seems a bit too high)

2.5.3 E734 at the Alternating Gradient Synchrotron (AGS) of the Brookhaven National Laboratory

- Both ν_μ and $\bar{\nu}_\mu$
- $\mu_{\nu_\mu} < 8.5 \times 10^{-10} \mu_B$

2.5.4 LSND

2.6 Direct electron (anti)neutrino magnetic moment measurements

2.7 Solar neutrino magnetic moment measurements

2.7.1 XENONnT

First results published in arXiv:2207.11330[?] on 22 July 2022.

- 5.9 tonne dual-phase liquid xenon TPC dark matter detector
- Region Of Interest is (1,140) keV
- Very low background (5 times lower than XENON1T)
- Tritium excluded as the potential background (also in XENON1T)
- No excess found - XENON1T excess excluded with 4σ
- The 90% C.L. upper limit on solar neutrinos with an "enhanced" magnetic moment is $\mu_{\nu_{sol}} < 6.3 \times 10^{-12} \mu_B$, the strongest non-astronomical limit so far (see fig.2)

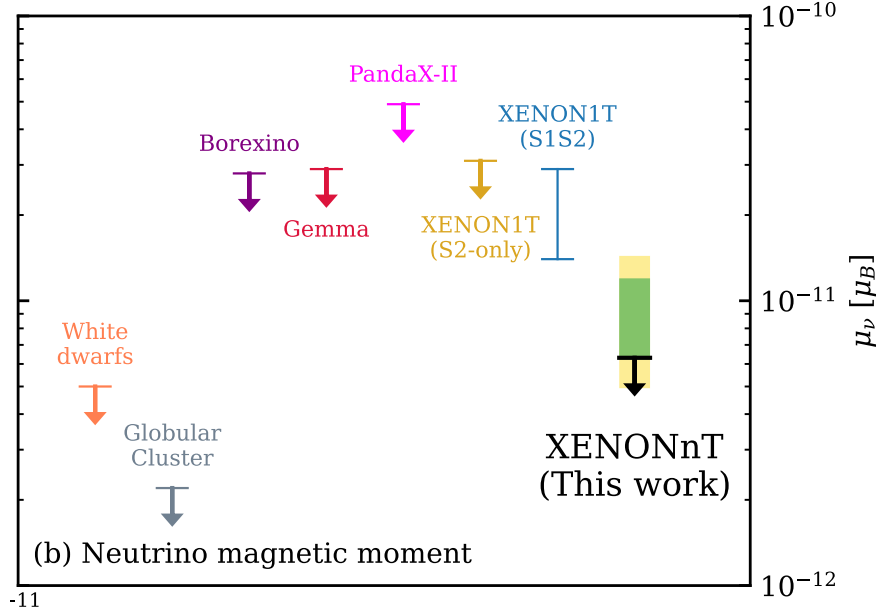


Figure 2: 90% C.L. upper limit on solar neutrinos with an enhanced magnetic moment.

Amir Khan used[?] XENONnT's results and derived limits on electromagnetic properties for the three SM neutrino flavours (see fig.3). For ν_μ they

2.7.2 XENON1T

2.7.3 BOREXINO

Should be $\mu_{\nu_e} < 2.8 \times 10^{-11} \mu_B$ [BorexinoLimit2017.pdf]

2.7.4 GEMMA

Should be $\mu_{\nu_{eff}} < 2.9 \times 10^{-11} \mu_B$. [GemmaLimits2013.pdf]

2.8 Other

2.8.1 LHC Forward Physics Facilities

Preliminary sensitivity studies for future experiments (namely for FLArE and FASERv2)

- LHC's Forward Physics Facilities study high energy (TeV) neutrinos of all flavours from the ATLAS interaction point.
- Large opportunity to study tau neutrinos in more detail

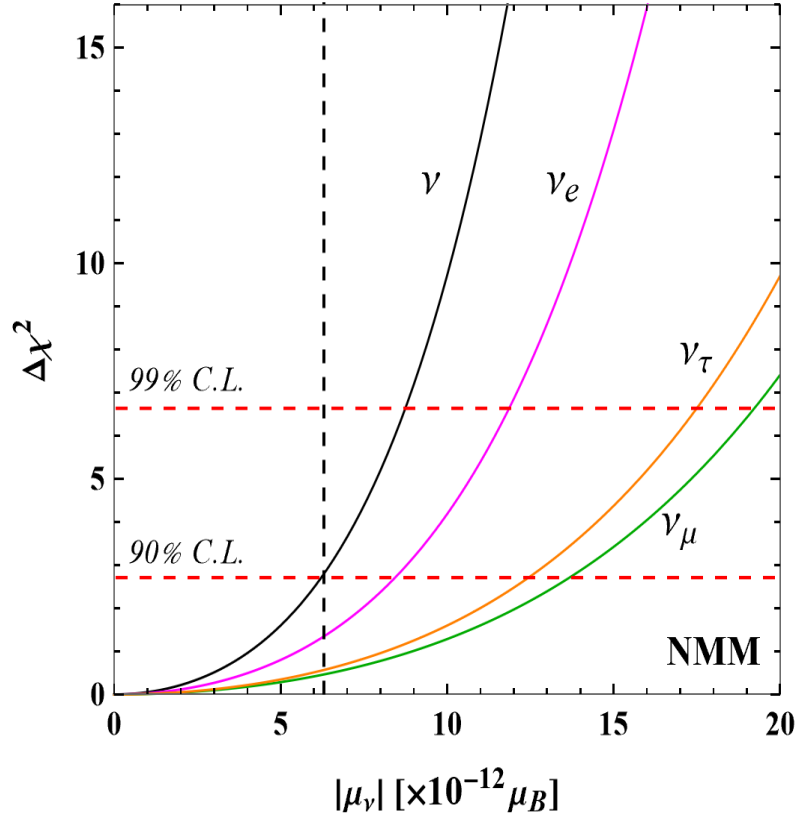


Figure 3: One-dimensional $\Delta\chi^2$ distribution with 90% and 99% C.L. boundaries of neutrino magnetic moments. The distribution in black corresponds to the effective flavor independent magnetic moment

2.9 Astrophysics

[NuMMBasicsAndAstro_2022.pdf] Neutrino electromagnetic processes that could be studied/observed in astrophysics

- Neutrino radiative decay
 - Decay of heavier neutrino flavour into a lighter neutrino and a photon
 - "The neutrino radiative decay has been constrained from the absence of decay photons in studies of the solar, supernova and reactor (anti)neutrino fluxes, as well as of the spectral distortions of the cosmic microwave background radiation."
 - Less stringent than the plasmon decay into a nu-antineu pairs
- Plasmon decay to neutrino-antineutrino pair
 - "For constraining neutrino electromagnetic properties, and obtaining upper bounds on neutrino magnetic moments in particular, the most interesting process is the plasmon decay into a neutrino-antineutrino pair [11]"
 - Plasmon decay frees the energy from the stars plasma in form of neutrinos that escape and therefore speeds up the star cooling
 - "observed properties of globular cluster stars provides new upper bounds on the effective neutrino magnetic moment $\mu_{ef} \leq (1.2 - 2.6) \times 10^{-12} \mu_B$ that is valid for both cases of Dirac and Majorana neutrinos."
- Transition of neutrino helicities $\nu_L \rightarrow \nu_R$ from active to sterile neutrinos
 - Supernovas would cool much faster - not observed for 1987A by Kamioka II and IMB, constraining Dirac neutrino mag. moment

3 Analysis overview

3.1 Datasets and Event Reconstruction details

3.1.1 Enhanced ν -on-e sample

3.1.2 Enhance ν_e CC MEC sample

3.2 Analysis weights

3.2.1 Neutrino magnetic moment as a weight

3.2.2 Radiative correction weight

3.3 Event selection

1. Very brief description of common-sense preselection cuts in decays
2. Description of all variables used for selection in this analysis
3. Plots of all variables used for selection in this analysis, showing the distribution with L: no cuts and R: cumulative cuts up to this point.
4. Test explaining the motivation for each selection cut.

Describe/point to the ND group's event selection Plots of event selection variables distribution with two columns. Left distribution with no cuts applied and right with all previous cuts applied.

3.4 Resolution and binning

3.4.1 Fitting framework

4 Systematic uncertainties

Plots showing combined uncertainties for signal and backgrounds

4.1 Normalization systematics

Should we include normalization systematics?

4.2 Neutrino flux systematics

Using the PCA vs using the PPFX universes+beam transport separately. Plots of energy showing shifts for signal and backgrounds separately

[to do]: understand differences with ND and 3F methods

4.3 Detector systematics

Plots of energy showing shifts for signal and backgrounds separately

4.4 Cross section systematics

Only for the non nu-on-e background. Assuming the nu-on-e events (including the signal events) are precisely known.

Plots of energy showing shifts for signal and backgrounds separately

5 Results

[to do]: talk about the shape-only versus normalisation-only strategies for the differential versus single-bin analyses.

5.1 Counting experiment

Single bin analysis - total numbers of signal and backgrounds

5.2 Binned experiment

Plots showing delta chi2 for stats and systs separately. Plot showing the chi2 with limits

5.2.1 Sensitivities and limits

6 Conclusion

Report the limit with its uncertainty.

Very briefly discuss differences with current world limit and how the techniques differ.

Very briefly summarise expectations for future measurements.